Cruz, R.; Correia, L.; Cabral-Fonseca, S.; Sena-Cruz, J. (2021) "Effects of the preparation, curing and hygrothermal conditions on the viscoelastic response of a structural epoxy adhesive." Adhesion and Adhesives, 110: 102961, 14 pp. DOI: 10.1016/j.ijadhadh.2021.102961

Effects of the preparation, curing and hygrothermal conditions on the viscoelastic response of a structural epoxy adhesive

Ricardo Cruz[1], Luís Correia[1], Susana Cabral-Fonseca[2], José Sena-Cruz[1*]

[1] University of Minho, ISISE, IB-S, Department of Civil Engineering, 4800-058 Guimarães, Portugal

[2] LNEC, National Laboratory of Civil Engineering, 1700-075 Lisboa, Portugal

[*]Corresponding author (jsena@civil.uminho.pt; Tel. +351 253 510 200; Fax +351 253 510 217)

Abstract

This paper addresses the viscoelastic behaviour of a commercially available cold-curing structural epoxy adhesive, under different preparation, curing and hygrothermal conditions. The main parameters studied were the preparation method (influence of the degassing and the temperature of the initial curing), the creep stress level, and the hygrothermal conditions. Tensile creep tests last up to 2400 hours. Test results revealed that the preparation method has great influence on the tensile properties of the adhesive, particularly on the viscoelastic response where degassing and curing at 20 ºC showed lower creep deformations. Specimens under 98% of relative humidity faced tertiary creep and then rupture. For the adopted levels of creep stress, the adhesive shows a linear creep behaviour, being parameterized using the Burgers and the modified Burgers equations.

Keywords: Epoxy adhesive; Viscoelasticity; Creep, Curing conditions

1. Introduction

The use of fibre reinforced polymer (FRP) materials for strengthening existing reinforced concrete (RC) structures has been constantly increasing during the past few decades [1,2]. Typically, FRP materials are externally bonded (EBR – Externally Bonded Reinforcement strengthening technique) or inserted into grooves opened on the concrete cover (NSM – Near Surface Mounted strengthening technique) of the elements to be strengthened [3]. FRP materials can be also applied in the prestressed state throughout the EBR or the NSM techniques. Several advantages have been appointed to the use of prestress, mainly because it combines the benefits of passive EBR or NSM FRP systems with the advantages associated

with external prestressing (deflection and crack width reduction, use of non-corrosive materials, more efficient use of the FRP materials, increase in the ultimate carrying capacity, among others) [4–6]. Epoxy adhesives, in particular cold-curing adhesives (able to cure under ambient temperature after the different components have been mixed), present a large variety of properties that make them suitable and very appealing for the bonding operation inherent to the EBR and NSM techniques, namely: (i) limited and low cure shrinkage; (ii) great compatibility with the concrete substrate and which allows good stress transfer between materials; (iii) good mechanical properties; (iv) wide range of operating temperature; (v) applicable in vertical surfaces, when presenting thixotropic characteristics; (vi) long open time; and (vii) good wetting properties for a variety of substrates. Bonding with epoxy adhesives can serve as an alternative to mechanical fasteners, which can be incompatible with several FRP systems [7–11].

The physical and mechanical properties of a cured epoxy are highly influenced by the curing conditions, in particular by the temperature, humidity and duration. Low temperature or excessive humidity can compromise the curing of the epoxy adhesive and undermine its performance and durability. In fact, extremely low temperatures (0 ºC) inhibited the curing from happening, whereas low temperatures (5 ºC to 10 ºC) may cause material vitrification and slowed down the curing process [11–13]. In contrast, elevated temperature accelerates the curing process of the epoxy adhesive. The adhesive's ability to cure fast at high temperatures has been used in the development of the gradient anchorage method, which is a non-mechanical anchorage used for prestressing EBR-FRP strips [4,8,14,15]. There are several advantages on using gradient anchorage method for FRP prestressing, namely the immunity to corrosion and the shorter duration for prestressing the FRP (finished after 3 hours). When compared with the ideal curing conditions (typically it last 3 to 7 days at 20 to 25 ºC, depending on the type of adhesive), accelerated curing with high temperature can lead to higher glass transition temperature [15]. Michels et al. [8] investigated the effect of different mixing and curing procedures on the mechanical performance of three different commercially available epoxy resins. The study included specimens subjected to accelerated curing (30 minutes at 90 ºC) and to curing under room temperature (21 ºC) for different periods of time (1 to 7 days). Specimens exposed to accelerated curing presented lower tensile properties (reduction up to 39% and 36% in strength and elastic modulus, respectively) and higher porosity when compared with specimens cured at room temperature. The porosity increased when the high temperature was applied, and it appears to be the cause for the apparent reduction on the tensile properties. The

authors also used a degassing mixer to minimize gas inclusion on the final mixture of the epoxy and, with it, observed a strong reduction on the porosity on both type of specimens (with and without accelerated curing). Specimens prepared with the degassing mixer presented the highest tensile modulus of elasticity (increase of 88% and 38% for accelerated curing and room temperature curing, respectively) and tensile strength (increase of 119% and 43% for accelerated and room temperature curing, respectively). Moussa et al. [12] investigated the influence of curing a cold-curing epoxy adhesive at low temperatures and a significant increase in the curing time was observed with lower temperatures; at high temperatures, in between 35 ºC to 60 ºC, few hours (3.7 to 1.6 h) were necessary to attain the full curing, whereas at a low temperature of 5-10 ºC, longer curing periods (3 days) were need. Moussa et al. [13] performed another investigation where an epoxy adhesive was cured at different isothermal temperatures (5 to 70 °C) during different curing periods. To evaluate the influence, the authors characterized the physical and mechanical properties of the adhesive. From the mechanical point of view, the development of tensile strength and stiffness *versus* time during isothermal curing rapidly increased at high curing temperatures, while a delay in the curing process was observed at low temperatures, mainly during the initial curing stage. Additionally, the authors concluded that the maximum stiffness was lower at 70 °C of curing temperature than at 25 °C. Savvilotidou et al. [16] studied the influence of curing level and exposure to humidity and alkalinity on the long-term physical and mechanical properties of an epoxy adhesive. The authors concluded that water uptake led to a reduction on the tensile E-modulus and tensile strength as a function of weight increase and immersion time. Additionally, the plasticization caused by the water uptake has changed the stress-strain curve of the specimens from initially almost linear to considerable non-linear. Moreover, there was a decrease in stiffness and strength, whereas the strain at failure increased.

In the context of FRP materials used in the EBR or NSM strengthening techniques, the knowledge on durability and long-term behaviour of the constituent materials is crucial. In particular, the creep behaviour of the bonding adhesive, which has been already recognized as one of the most relevant properties to guarantee proper stress transfer in a bonded joint over time [10]. When exposed to sustained stress, epoxy adhesives typically present relevant creep deformation, which are strongly affected by the loading age, stress level and exposure conditions (temperature and humidity) [7,10]. Costa and Barros [10] carried out a study on the tensile creep behaviour of a commercially available epoxy adhesive used

for construction. Specimens were loaded with a constant stress of 20%, 40% and 60% of the adhesive's tensile strength, for a period of 1000 hours, under controlled environment (20 ºC and 60% of relative humidity). The epoxy adhesive presented a linear viscoelastic/viscoplastic behaviour up to the maximum stress level (60% of the tensile stress), parameterized using the modified Burgers model. It is noteworthy to mention that the specimens were loaded with 3 days of curing, for which the authors agreed to be enough time of curing to reach the adequate bond strength to concrete and to stabilize the tensile strength and elastic modulus.

In prestress applications with EBR-FRP strips, the epoxy adhesive might be subjected to sustained stress at early ages (after 24 hours) [4,5]. In this context, it is essential to understand the creep behaviour of the adhesive at early stages, because excessive creep can compromise the effectiveness of the prestress application [10]. Silva et al. [7] performed an experimental tensile creep test with epoxy adhesive, since its early ages. Epoxy specimens were exposed to (i) two different creep load levels (30% and 40% of the tensile strength) at (ii) four different loading ages (1, 2, 3, and 7 days). In agreement with Costa and Barros [10], Silva et al. [7] observed a significant development of the instantaneous tensile properties (modulus and strength) up to the 3 days of age, for which the rate of increase of stiffness slowed down and stabilized. The creep coefficient (ratio of the creep and instantaneous deformations/strain) decreased with the age of loading, being equal to 4.1, 2.1, 1.9 and 1.3 for specimens loaded at the ages of 1, 2, 3, and 7 days, respectively. The results showed that the curing of the adhesive, specifically the formation of cross-links of the polymer chains, continued to occur during the creep loading, which led to similar post-unloading phase between all specimens. Results also showed that the epoxy presented linear viscoelastic behaviour up to the maximum stress level (40% of the tensile stress). With an unsuccessful attempt to simulate the creep behaviour of epoxy adhesive in early ages with the modified Burgers model, the authors presented a new framework based on the generalized Kelvin model, with excellent fit to the experimental results since the early ages (1 day of curing), in both the loading and recovery phase of the creep tests.

The long-term behaviour of an adhesive can be compromised by the environmental conditions to which it is exposed. Therefore, research has been carried out to evaluate the durability of epoxy adhesives, namely the most severe environments, degradation mechanisms and the effect of such environments have been reported [9,11,17]. Cabral-Fonseca et al. [11] presented an exhaustive literature review on the

durability of FRP-concrete bonded joints, with a great focus on the durability of the adhesive in several environments (water/moisture, temperature, freeze-thaw, chemical environments, UV radiation, and fire). According to their literature review, exposure to moisture can result in reversible degradation processes such as swelling and plasticization and, with time, to irreversible processes like chemical degradation, micro cracking and chain scission. Temperature can influence the propagation of moisture and potentiate the degradation process on epoxy resins. Therefore, the hygrothermal conditions have great influence on the long-term properties of epoxy adhesive and, consequently on FRP-concrete bonded joins. The experimental work and literature review carried out by Sousa et al. [9] and Silva et al. [17] on the durability of epoxy adhesives for construction sector subjected to different hygrothermal environments supports the former statement. In both studies, a generalized decrease on the on the glass transition temperature and on the tensile properties was detected. Both authors observed that a less severe degradation occurred for specimens immersed in saltwater, than in regular water. Additionally, Silva et al. [17] noted that specimens subjected to thermal cycles showed an increase on the tensile properties (up to 15% and 33% on the modulus and ultimate strength, respectively) due to a post-curing event motivated by the exposure to high temperatures.

In spite of these recent studies on epoxy resins typically used for RC strengthening with FRP materials, the existing knowledge about its durability is still scarce. Moreover, the effect of different mixing and curing conditions on the long-term behaviour of such adhesives is unknown. Epoxy adhesives commonly used in EBR-FRP prestress applications are continuously subjected to a stress state face environment where the effect of moisture and temperature is also unknown and can be relevant.

This study intends to extend the existing knowledge namely in the following topics: (i) creep behaviour of epoxy adhesives manufactured with degassing and accelerated curing; (ii) influence of the relative humidity on the creep behaviour of epoxy adhesives prepared with distinct processes; and (iii) suitability of existing models to simulate the creep behaviour of epoxy adhesives prepared using different processes. Therefore, this work aims at assessing the tensile creep behaviour of a commercially available epoxy-based structural adhesive (traded under the name "S&P Resin 220"), used for bonding Carbon FRP (CFRP) to concrete throughout the EBR and NSM techniques. This epoxy has been also used for EBR-FRP prestress applications, therefore specific focus was given to the preparation and curing conditions and to the effect of the hygrothermal conditions under creep stress. The experimental work

included the following variables: (i) three distinct preparation procedures; (ii) two creep stress levels; and (iii) two different hygrothermal conditions.

This paper presents the results of an experimental work were the tensile mechanical properties and the viscoelastic behaviour of a commercially available cold-curing structural epoxy adhesive. Three different preparation methods (application or not of degassing during mixing and of high temperatures during the curing) were considered during samples manufacturing. Tensile tests after 7 days were performed. Then, tensile creep tests were conducted, varying the creep stress level and the hygrothermal conditions up to 2400 hours. The linear creep behaviour observed for the adopted levels of creep stress, was parameterized using the Burgers and the modified Burgers equations.

2. Experimental programme

2.1. The epoxy adhesive studied

The 'S&P Resin 220 epoxy adhesive' was studied in the present investigation. It is a commercially available epoxy adhesive widely used in retrofitting reinforced concrete structures with FRP laminate strips. This structural epoxy is a grey two-component mix, where the component A (Bisphenol A based resin, light grey colour) is mixed with the component B (hardener, black colour) with the ratio of 4:1 (Component A: Component B). This epoxy adhesive is solvent free, thixotropic and, after mixing the two components, presents the density of 1.70 – 1.80 [g/cm^3]. According to the supplier, after 3 days of curing at 20 ºC, this epoxy adhesive should present the following mechanical properties [18]: (i) compressive strength >70 MPa (EN 12190:1999 [19]); (ii) flexural E-modulus >7.1 GPa (EN ISO 178:2002 [20]); (iii) shear strength >26 MPa (EN 12615:1999 [21]).

2.2. Specimens, test setup and methods

Specimens were prepared with Teflon moulds in which the mixed compound was filled in. Each specimen was produced according to "type 1A" defined in EN ISO 527-2:2012 [22], with a total length of 170 mm and a thickness of 4 mm, in a dogbone shape (see Figure 1a). In total, 60 specimens were prepared, 24 of them were used to assess the instantaneous mechanical tensile properties while the remaining 36 specimens were used to study the tensile creep behaviour. Three batches were used for manufacturing of the epoxy specimens, each one planned for studying the effect of a specific set of

hygrothermal conditions on the viscoelastic response of the adhesive. The preparation of the epoxy specimens was carried out using three different preparation methods and curing conditions:

i. REF method, in which the epoxy adhesive was prepared following the instructions of the supplier [18]: first, each component was separately stirred; then component A was mixed with the component B with the weight ratio of 4:1; the compound was thoroughly and slowly manually mixed until the colour was uniformly grey and free of any streaks; the mixing process lasted approximately 4 minutes. Afterwards, the uniform mixture was poured into the Teflon moulds. Then, an acetate sheet was placed on the top surface and pressed with a steel roller, thus ensuring the correct thickness. The specimens were demoulded after 24 hours and kept in a climatic chamber at 20 (±2) °C of temperature and 55 (±2)% of relative humidity (20 °C / 55% RH), for 7 days before testing;

ii. V20 method, in which the mix process involved degassing in order to minimize the gas inclusion in the final mixture (see Figure 2). The mix process was identical to the adopted process for REF specimens, with the inclusion of degassing during the mixing. V20 specimens were also kept in a climatic chamber at 20 °C / 55% RH, for 7 days before testing;

iii. V90 method, in which the initial step of mixing and degassing used in V20 specimens was also adopted. However, just after casting on the Teflon moulds, these specimens were subjected to an accelerated curing process, exposing them to a temperature of 90 (±2) ºC during 30 minutes. Then, the specimens were kept for 7 days at 20 °C / 55% RH, in a climatic chamber.

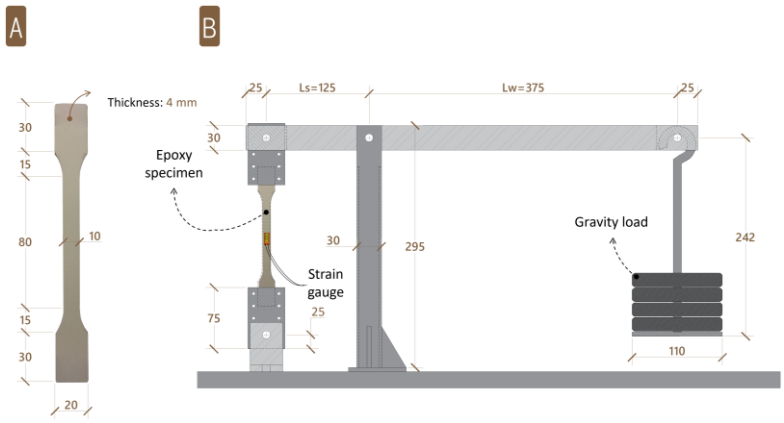

Figure 1. (a) Tensile test specimen's geometry; (b) tensile creep test setup. All units in [mm].

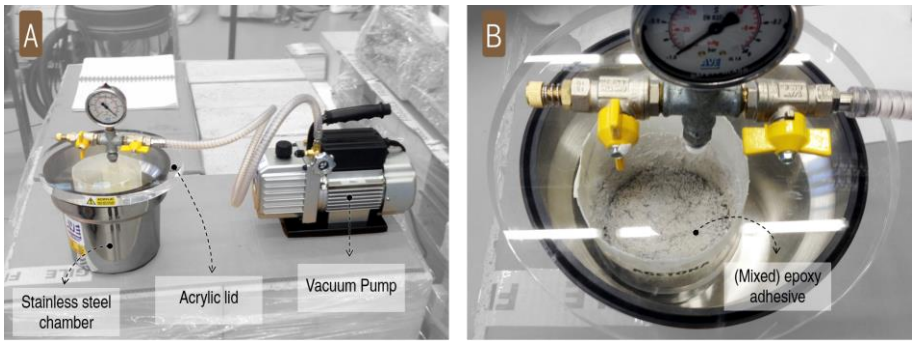

Figure 2. (a) Vacuum system; (b) degassing of mixed epoxy adhesive components.

195

196 The tensile properties of the epoxy adhesive were assessed throughout the standard ISO 527-1:2012 [23].
197 The tensile tests were carried out in a universal testing machine under displacement control of 1 mm/min
198 (see Figure 3a). The applied load was measured using a load cell with 10 kN of maximum capacity
199 (linearity error less than ± 0.05%) and the axial strain was measured using a clip gauge with a base length
200 of 50 mm (precision of ±1 μm) placed at the middle specimen height. Prior performing the tensile tests,
201 the thickness and width of all specimens was assessed using a digital calliper (0.01 mm of precision) in
202 three different sections (one at middle height and two at 25 mm apart to the former). In total, 24
203 specimens were tested, eight for each type of preparation method (see Table 1). The tensile creep
204 properties were assessed using a mechanical system based on a lever structure [7,10], schematically
205 represented in Figure 1b, where each epoxy specimen was subjected to constant stress throughout
206 application of a predefined gravity load (see Figure 3b). A total of 18 specimens were submitted to a
207 constant tensile stress for a minimum period of 100 days (2400 hours). These specimens were grouped
208 in the following three series:

209 i. EP1 series (composed of 6 specimens: 2 REF, 2 V20 and 2 V90), where specimens were
210 subjected to a creep load equal to 40% of the adhesive's tensile strength, in a controlled
211 environment characterized by 20 °C / 55% RH;
212 ii. EP2 series (composed of 6 specimens: 2 REF, 2 V20 and 2 V90), where specimens were
213 subjected to a load of 30% of the adhesive's tensile strength in the same environmental
214 conditions as specimens from series EP1;
215 iii. EP3 series (composed of 6 specimens: 2 REF, 2 V20 and 2 V90), where specimens were
216 subjected to a creep load equal to 30% of the adhesive's tensile strength, and to the hygrothermal
217 conditions of 20 °C / 98% RH.

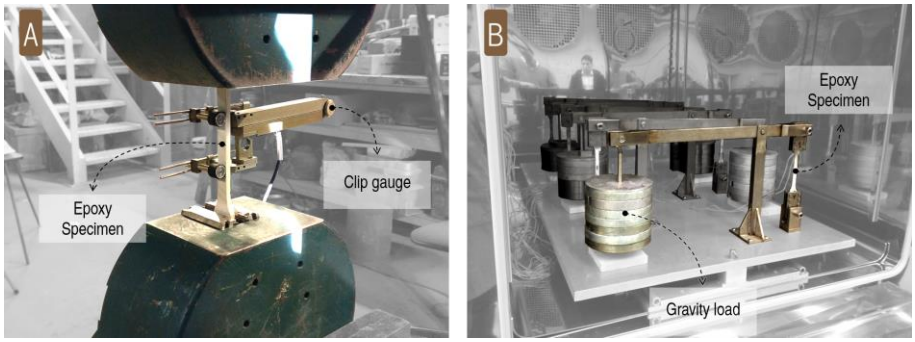

Figure 3. Test setup for (a) tensile tests; (b) tensile creep tests in the climatic chamber.

To secure the referred environmental conditions, a climatic chamber FITOCLIMA 1500EC45 (temperature range: -45 ºC to 180 ºC; humidity range: 10% to 98%) was used. In the creep test program, the specimens were labelled according to the following mask X_Y_Z, where the variables are: X stands for the series (EP1, EP2, and EP3); Y corresponds to the preparation method (REF, V20, and V90); and Z is used to differentiate specimens from the same series and preparation method (1 and 2). The instrumentation included two strain gauges with a 5 mm measuring length (type BFLA-5-3-3L from TML) installed precisely at the middle height of each face (see Figure 1b). The data was acquired at frequency of 1 Hz during the first hour of loading, followed by 16,67 Hz (one record per minute) during 2 hours, and finally 1,67 Hz (one record every 10 minutes) until the end of the test. Nine "dummy" specimens were also manufactured (3 for each series, where each specimen was prepared according to the preparation methods described above) and instrumented with one strain gauge to measure possible environmental effects on the material and on the strain gauge wires. Nine additionally specimens were used in EP3 series (three specimens for each preparation method) to measure the mass variation. The tensile tests and the creep loading were always conducted 7 days after the adhesive preparation.

233 **Table 1:** Results of tensile tests.

Preparation Method	Series [(1)]	Specimen	f_{ult} [MPa]	E_{adh} [GPa]	ε_{ult} [%]
REF *1. Manual mixing* *2. Curing at 20 °C and 55% RH for 7 days*	EP1	REF_1	21.5	7.65	0.48
		REF_2	20.4	7.39	0.39
		REF_3	20.5	7.67	0.34
		REF_4	23.0	7.67	0.59
	EP2	REF_5	24.4	7.88	0.55
		REF_6	23.2	8.11	0.32
		REF_7	21.8	7.98	0.27
		REF_8	21.2	8.16	0.25
		Average	**22.0 (6.02%)**	**7.81 (3.16%)**	**0.40 (29.91%)**
V20 *1. Manual mixing + degassing* *2.Curing at 20 °C and 55% RH for 7 days*	EP1	V20_1	29.5	11.12	0.31
		V20_2	28.1	11.31	0.27
		V20_3	25.4	11.11	0.23
		V20_4	29.0	11.24	0.29
	EP2	V20_5	30.0	11.15	0.26
		V20_6	30.3	10.86	0.30
		V20_7	28.4	10.48	0.28
		V20_8	30.3	10.70	0.33
		Average	**28.9 (5.25%)**	**11.00 (2.45%)**	**0.28 (10.40%)**
V90 *1. Manual mixing + degassing* *2. Accelerated curing at 90 °C for 30 min* *3. Curing at 20 °C and 55% RH for 7 days*	EP1	V90_1	31.5	12.96	0.25
		V90_2	31.3	12.02	0.27
		V90_3	31.4	12.01	0.27
		V90_4	32.6	11.54	0.30
	EP2	V90_5	29.9	11.04	0.27
		V90_6	33.5	11.22	0.37
		V90_7	33.6	11.30	0.35
		V90_8	31.5	10.96	0.31
		Average	**31.9 (3.58%)**	**11.63 (5.39%)**	**0.30 (13.27%)**

Notes: [(1)] Tests were conducted 7 days after casting – specimens from EP1 and EP2 series were manufactured/tested in distinct dates (only one batch per series); the values between parentheses are the corresponding coefficient of variation.

234

235

3. Results and discussion

3.1. Tensile properties

The stress-strain curves obtained from the tensile tests are presented in Figure 4a, while the tensile strength (f_{ult}), the elastic modulus (E_{adh}) and the ultimate strain (ε_{ult}) are graphically presented throughout boxplot diagrams in Figure 4b. Table 1 presents the main parameters obtained from the tensile tests.

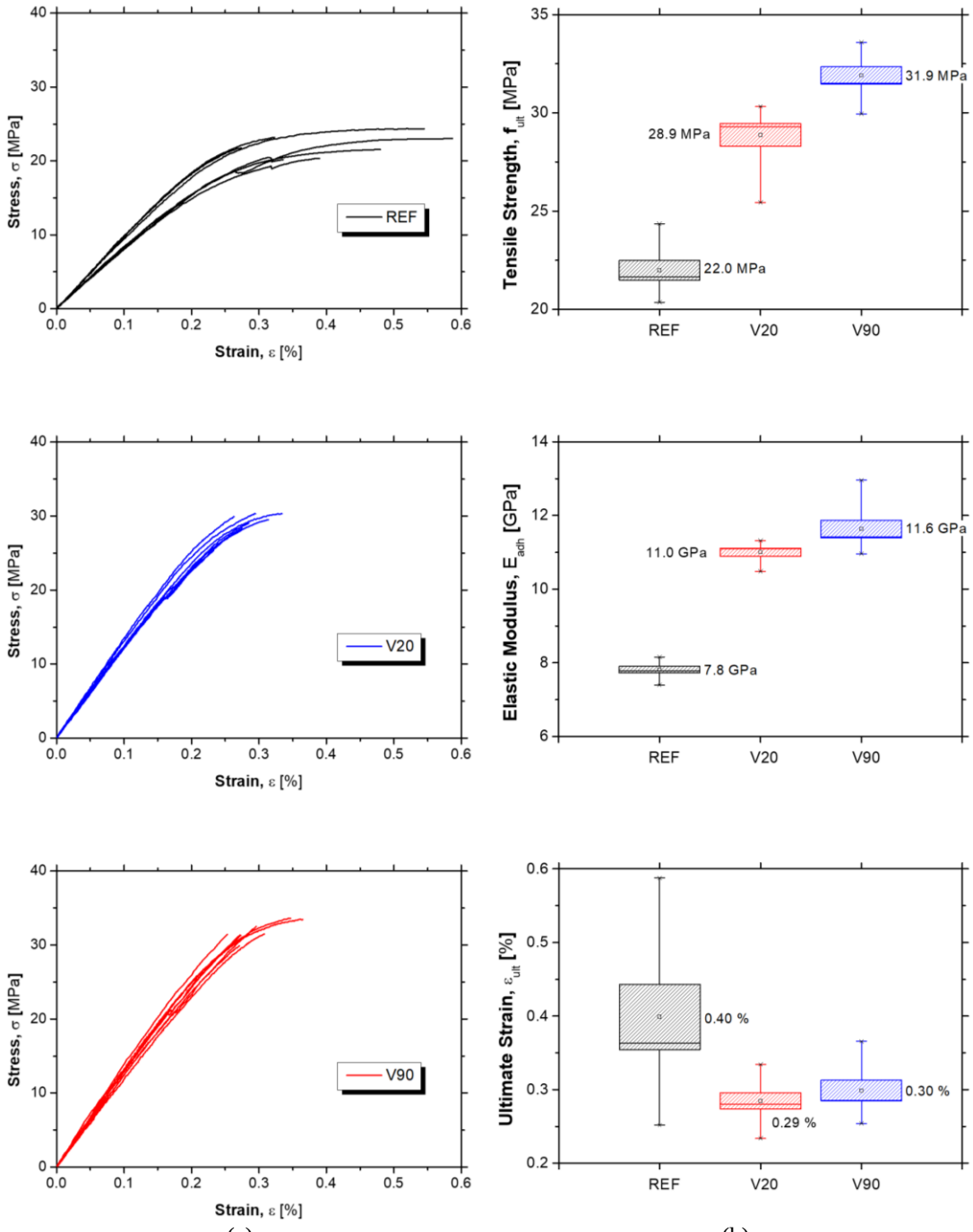

Figure 4. (a) Experimental tensile stress *versus* strain curves; (b) boxplot representation of the tensile strength, elastic modulus and ultimate strain. Notes: the square point is the mean value, the bottom

and top lines of the box plot are the 25th percentile and 75th percentile, the line inside the box is the median and the vertical line is whisker boundaries.

Results in Figure 4a show that the preparation method has great influence in the mechanical properties of the epoxy adhesive, namely that the degassed specimens (V20 and V90) exhibited a clear increase on the tensile strength and elastic modulus and decrease on ultimate strain, when compared with REF specimens. The tensile properties, E_{adh}, f_{ult}, and $\varepsilon_{\mathrm{ult}}$, obtained in REF specimens are equal to 7.81 GPa (CoV=3.16%), 22.0 MPa (CoV=6.02%), and 0.40 % (CoV=29.91%), respectively. Because this epoxy adhesive is commercially available, several authors have already characterized the tensile properties, e.g. [7,8,10,17,24], and their results are in agreement with the ones obtained during this study (regarding the REF preparation procedure). When compared with the REF specimens, the V20 specimens presented an increase on the average tensile strength and elastic modulus of 31% and 41%, respectively, whereas the V90 specimens show an even higher growth on f_{ult} and E_{adh} of 45% and 49%, respectively. The increase on these two parameters was expected in degassed specimens, since the vacuum process drastically reduces the quantity of pores (created by the existence of air and volatiles). According to Michels *et al.* [8], the porosity values of ~2.5% to 3.5% can be found in normal epoxy mixing by hand followed by curing at room temperature, while specimens that undergo degassing process have porosity values of ~0.5%. The same authors also realized that curing at higher temperatures (80 ºC to 90 ºC for 25 minutes), led to faster development of strength and stiffness and it might cause an increase on the porosity ratio. In the present study, results show an increase on the tensile strength and elastic modulus of specimens prepared with the V90 method, when compared with the V20 (see Table 1 and Figure 4b). The boxplot diagrams presented in Figure 4b shows the dispersion on the results of each method of preparation and supports the influence between the preparation method and the mechanical performance of the epoxy. Figure 4b also presents the average value for each studied parameter. In average the ultimate strain on the REF specimens was greater than on V20 and V90 specimens. It is, however, noteworthy to mentioned that the ultimate strain observed on REF specimens exhibit the greatest dispersion of results. In all the three evaluated parameters (E_{adh}, f_{ult}, and $\varepsilon_{\mathrm{ult}}$), the lowest dispersion of results was observed on degassed specimens cured at room temperature, followed by the specimens subjected to accelerated curing at 90 ºC.

3.2. Tensile creep behaviour

As introduced before, the assessment of the tensile creep properties of the epoxy adhesive was carried out throughout three series of tests, each one composed of 6 specimens. The main variables in the study were (i) the preparation procedure; (ii) the creep load; and the (iii) hygrothermal conditions. For each series, three "dummy" specimens (each one with a different preparation procedure) were instrumented with one strain gauge to measure the other effects, namely (i) epoxy curing effects due to hygrothermal conditions and (ii) thermal effect on the measuring system (sensors, wires, etc.). Figure 5 shows the typical evolution of strain with the time observed on the "dummy" specimens – EP2_V20 ("Dummy") – , on the creep specimens – EP2_V20_1 (Original) –, and the result when the strain value from the "dummy" specimen is subtracted from the creep specimen – EP2_V20_1 (Final). As can be seen in Figure 5, the strain variation overtime in the control specimen could not be neglected and, therefore, the strain measured in the test specimens was rectified based on the measurements from the control specimens manufactured with the same preparation procedure. In general, the "dummy" specimens showed a constant strain increase (expansion) of 0.002% of strain and 0.005% of strain every 100 days, for the environments with 50% RH and 98% RH, respectively. After 2400 hours, the average 0.048% of strain measured on the "dummy" specimens subjected to 55% RH represented, approximately 14% and 16% of the total strain registered in the "original" specimens from EP1 series (load equal to 40% of the adhesive's tensile strength) and EP2 series (load equal to 30% of the adhesive's tensile strength), respectively. Although the strain increase on the "dummy" specimens from EP3 series (98% RH) was the highest, it represented, in average, 17% of the total strain registered in the "original" specimens at failure. It should be noted that in EP3 series, the failure typically occurred before 2400 hours. Also, the strain was registered at the end of the test, with the full development of the primary, secondary and tertiary creep stages. Therefore, the abovementioned ratio between "dummy" strain and "original" strain cannot be directly compared between series. It should be also noted that within each series, the "dummy" strain observed on specimens prepared with the degassing procedure (V20 and V90) presented slightly lower values than the reference specimens (REF). This observation reveals that the degassing procedure might led to greater water uptake resistance. For the EP3 series, the kinetic of the "dummy" strains is similar to the mass variation depicted in Figure 9, due to water uptake, being much higher in REF than in V20 and V90 series. Furthermore, swelling effects may justify such level of strains. Additional curing

298 of specimens along the time can result in negative strains due to densification, but the swelling effect can
299 lead to higher expansion, which can compensate the former effect.

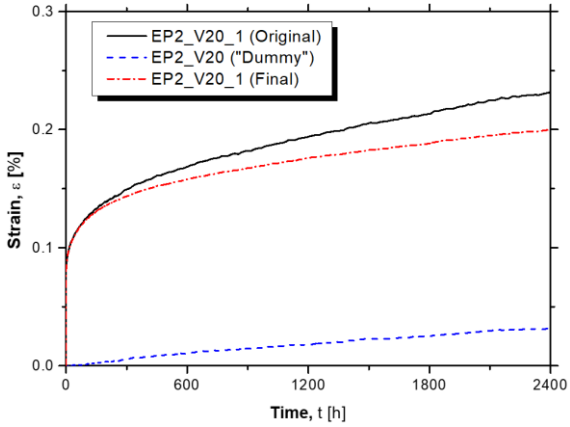

Figure 5. Typical strains measured in tested and "dummy" specimen.

300

301 Based on the abovementioned correction, the creep strain curves were plotted and are presented in
302 Figure 6. Per specimen, this figure presents (i) the envelope of the strain overtime measured in both
303 monitored faces and (ii) the average strain. The largest difference between the strain gauges recorded
304 from the opposite faces was registered on specimens EP2_REF_2 (smaller than 0.1% of strain). It is
305 noteworthy that in the case of specimens EP2_REF_1, EP2_V20_2, EP3_REF_1, EP3_REF_2,
306 EP3_V20_1, and EP3_V20_2 only one strain gauge was used since the other sensor faced technical
307 issues and, thus, had to be disregarded. To facilitate the analysis of the tensile creep results, Figure 7
308 presents the average strain *versus* time and average creep compliance *versus* time. Table 2 shows the
309 main parameters extracted from the creep strain curves.

310

311 **Table 2:** Results of tensile creep tests and curve parameters.

Series	Specimen	σ_{creep} [MPa]	ε_{t0} [%]	$E_{(t=0)}$ [GPa]	$\varepsilon_{t=2400}$ [%]	$J_{t=2400}$ [1/GPa]	t_{rup} [h]	$\Delta\varepsilon_{rup}$ [%]	E_{rup} [GPa]	$\varphi_{t=2400}$
ηEP1	EP1_REF_1	8.74	0.10	8.78	0.37	0.43	--	--	--	2.72
	EP1_REF_2	8.55	0.10	8.37	0.34	0.40	--	--	--	2.33
	EP1_V20_1	11.6	0.09	12.4	0.32	0.28	--	--	--	2.43
	EP1_V20_2	11.2	0.09	12.2	0.28	0.25	--	--	--	2.03
	EP1_V90_1	12.8	0.11	12.0	0.32	0.25	--	--	--	1.98
	EP1_V90_2	12.8	0.10	12.6	0.33	0.26	--	--	--	2.28
EP2	EP2_REF_1	6.87	0.08	9.00	0.29	0.42	--	--	--	2.77
	EP2_REF_2	6.86	0.07	9.91	0.23	0.33	--	--	--	2.32
	EP2_V20_1	8.91	0.07	13.3	0.20	0.22	--	--	--	1.99
	EP2_V20_2	8.90	0.07	13.7	0.20	0.22	--	--	--	2.06
	EP2_V90_1	9.63	0.07	13.2	0.21	0.22	--	--	--	1.91
	EP2_V90_2	9.64	0.08	12.9	0.23	0.24	--	--	--	2.08
EP3	EP3_REF_1	7.32	0.10	7.36	0.57 (1)	0.78 (1)	2112.5	-0.10	7.20	4.73 (1)
	EP3_REF_2	5.60	0.10	8.14	0.56 (1)	0.69 (1)	1475.5	-0.12	7.02	4.59 (1)
	EP3_V20_1	4.55	0.08	11.5	0.46 (1)	0.48 (1)	3627.5	-0.09	10.46	4.48 (1)
	EP3_V20_2	--	--	--	--	--	--	--	--	--
	EP3_V90_1	3.78	0.08	13.2	0.38 (1)	0.36 (1)	1977.0	-0.09	12.00	3.72 (1)
	EP3_V90_2	4.30	0.08	13.2	0.43 (1)	4.25 (1)	2123.5	-0.09	11.58	4.25 (1)

σ_{creep} – creep stress; $\varepsilon_{(t=0)}$ – instantaneous elastic strain at the instance of loading (t = 0 h); $E_{(t=0)}$ – Modulus of elasticity based on the instantaneous deformation; $\varepsilon_{(t=2400)}$ – strain registered after 2400 h of creep loading; $J_{(t=2400)}$ – creep compliance for 2400 h; t_{rup} – time of failure; $\Delta\varepsilon_{rup}$ – instantaneous strain variation after rupture; E_{rup} – Modulus of elasticity based on the instantaneous strain variation after rupture; $\phi_{(t=2400)}$ – creep coefficient.

Note: (1) Value obtained at rupture

312

313

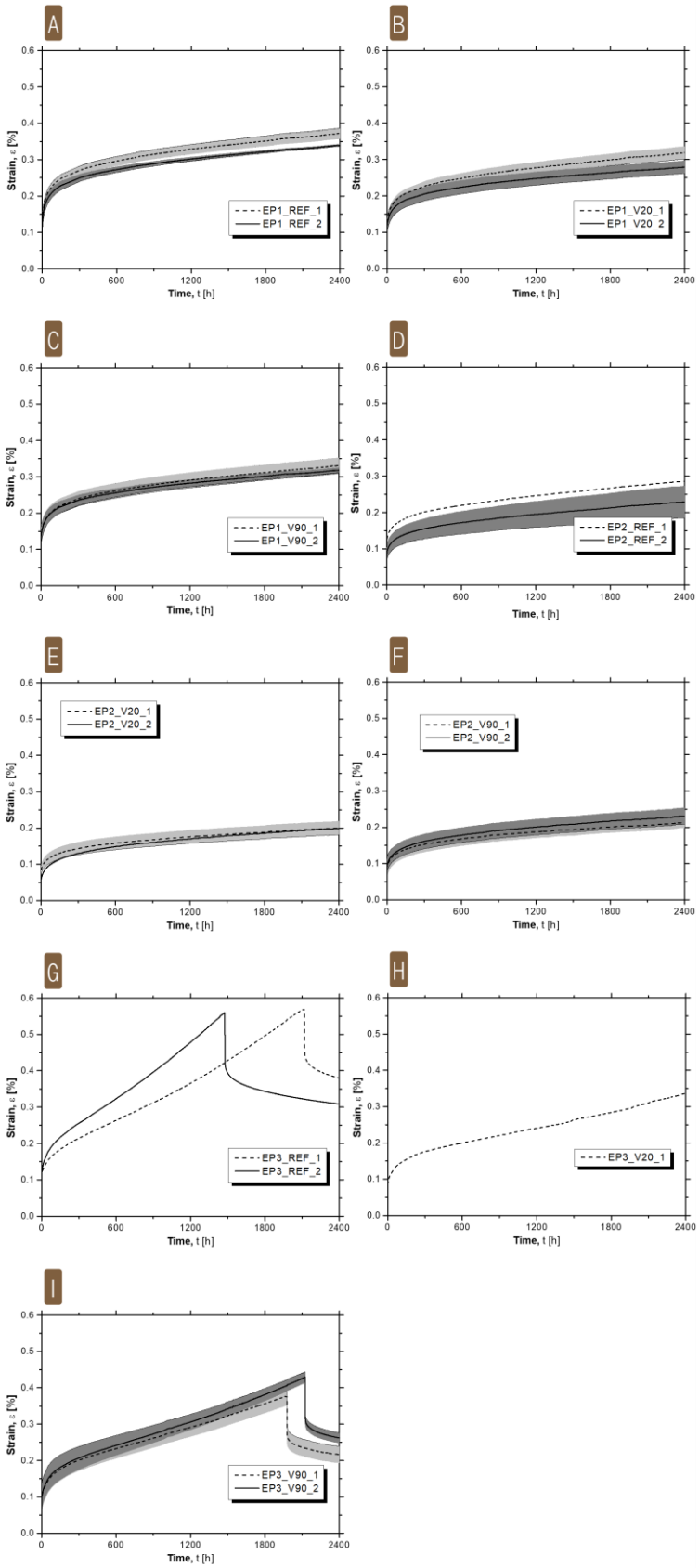

Figure 6. Strain *versus* time for the tested series (envelopes): (a) to (c) EP1 series; (d) to (f) EP2 series; (g) to (i) EP3 series.

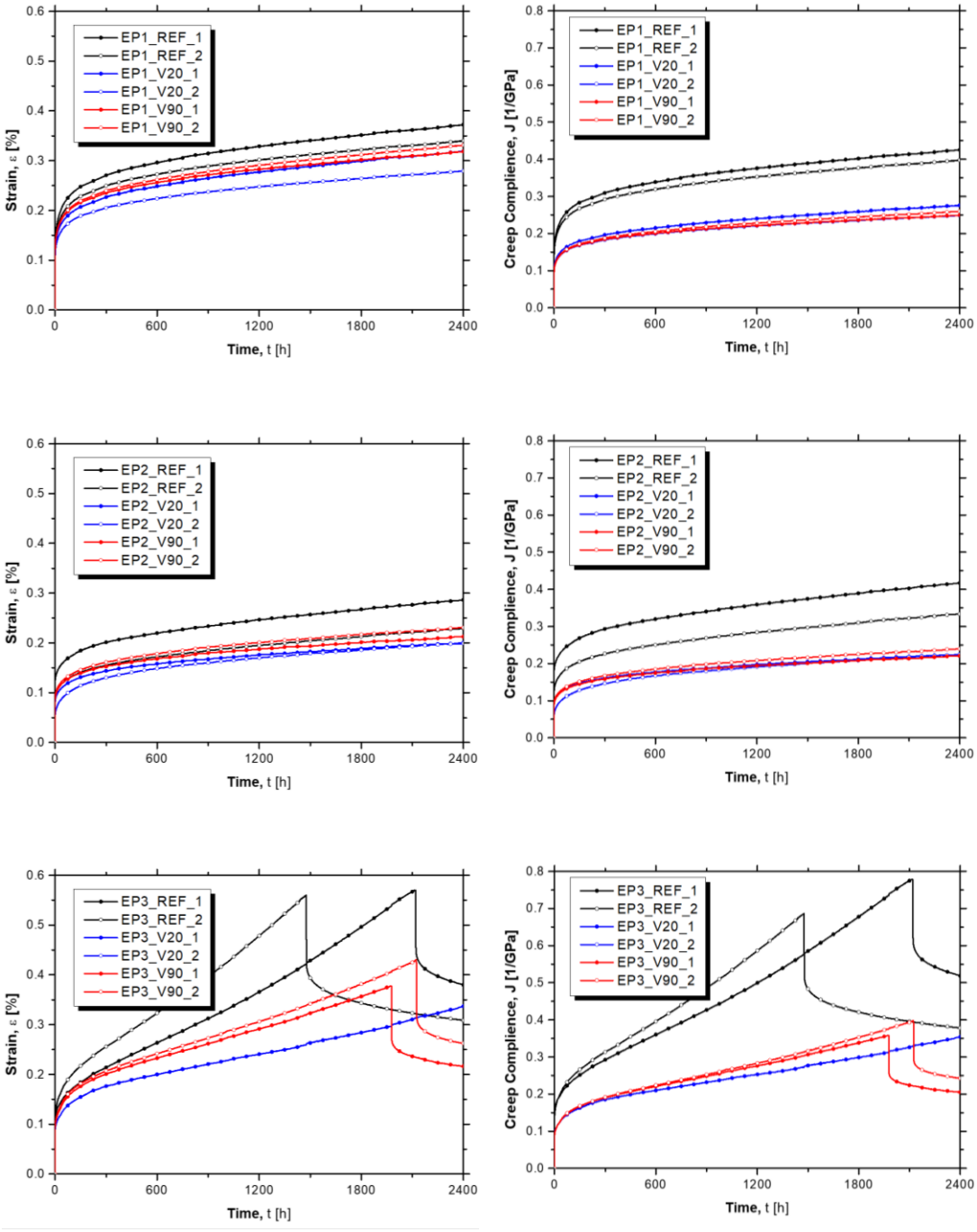

Figure 7. (a) Strain *versus* time and (b) creep compliance *versus* time all the tested specimens.

The modulus of elasticity, $E_{(t=0)}$, based on the instantaneous elastic strain observed at the moment of loading, $\varepsilon_{(t=0)}$, was computed for all creep specimens (see Table 2). REF, V20 and V90 specimens presented the average value of 8.59 GPa (CoV=9.2%), 12.6 GPa (CoV=6.2%), and 12.8 GPa (CoV=3.5%), respectively. These values are slightly higher (~12%) than the modulus of elasticity, E_{adh}, obtained in the tensile tests according to ISO 527-1:2012 [23]. It is noteworthy that the latter values are

computed throughout the secant modulus between strain 0.05% and 0.25% of the stress-strain curves, whereas the elastic strain, $\varepsilon_{(t=0)}$, was typically inferior to 0.1%.

Results clearly show that the hygrothermal conditions (EP2 *versus* EP3 series) had major influence on the adhesive's creep behaviour (see Figures 6 and 7). Similar behaviour between EP1 and EP2 series (kept at 20 ºC and 55% of relative humidity) was observed, with the development of primary creep within the first 500 hours, followed by a secondary creep stage until the end of the test. Specimens from EP3 series (kept at 20 ºC and 98% of relative humidity) experienced the three stages of creep (primary, secondary and tertiary) followed by fracture. It should be noted that in EP3 series, significant differences were observed between specimens manufactured with different methods (REF, V20 and V90): in EP3 series, specimens prepared with the REF method, exhibit the highest creep strain (at failure, equal to 0.57% and 0.56% for EP3_REF_1 and EP3_REF_2, respectively), with the primary creep being develop in the first 200 hours, secondary creep stage in the following 600 – 800 hours, and, lastly, the tertiary creep stage (rupture occurred after 2116 hours and 1476 hours of test for specimens EP3_REF_1 and EP3_REF_2, respectively); in contrast, the specimen EP3_V20_1, manufactured with the V20 preparation method (EP3_V20_2 had to be disregarded due to malfunction of the strain gauges), presented the slowest creep development, with the failure occurring after 3628 hours for a strain value of 0.45%, and with the complete development of the primary and secondary creep stages within the first 400 hours and 1500 hours, respectively; lastly, the V90 specimens exhibit the primary (within the first 300 hours), secondary (duration of 700 hours) and tertiary (until rupture at 1977 hours and 2124 hours, for specimens EP3_V90_1 and EP3_V90_2, respectively) stages, with the maximum strain of 0.43% registered in specimens EP3_V90_2. The creep coefficient, $\varphi_{(t=2400)}$, was computed as the ratio between the increment of creep strain ($\varepsilon_{(t=0)}$-$\varepsilon_{(t=2400)}$) and the instantaneous strain ($\varepsilon_{(t=0)}$) at the onset of the creep loading, and the obtained values are presented in Figure 8. The creep coefficient was computed after 2400 hours of loading, with exception to EP3 series, where the maximum attained strain value was considered because failure was typically observed before the predefined time period. Again, EP1 and EP2 series presented similar creep coefficients. More specifically, specimens prepared according to the REF method, presented creep coefficient of 2.53 and 2.55 for EP1 and EP2 series, respectively. The $\varphi_{(t=2400)}$ for the V20 and V90 specimens was in average equal to 2.23 and 2.13, respectively, for EP1 series and equal to 2.03 and 2.00, respectively, for EP2 series. These similarities between EP1 and EP2

series (see Figure 7b and Figure 8) revealed that this epoxy adhesive can be assumed as linear viscoelastic material, for creep stress levels used. Other authors [7,10] have also observed the same property for this epoxy adhesive. In contrast, EP3 series presents creep coefficients significantly higher, mainly because the hydrothermal conditions led to the development of tertiary creep stage and rupture, within the first 2400 hours. The creep coefficient in these specimens was computed for the test period, using the last value of strain before the specimen's failure. The differences in the creep coefficients (were 88%, 111% and 93% higher than in EP1 and EP2 series, for the REF, V20 and V90 methods, respectively) are clearly shown in Figure 8.

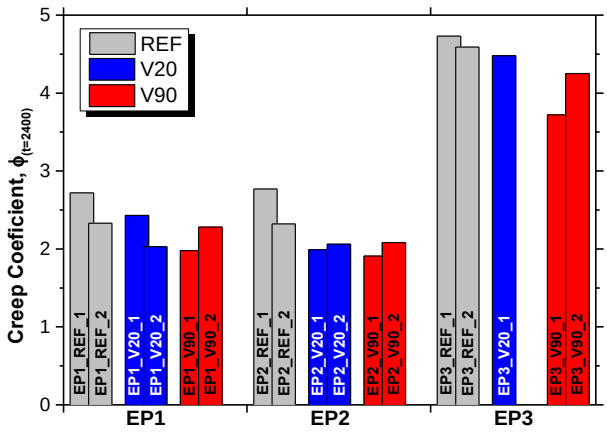

Figure 8. Creep coefficient for all tested specimens

It is state-of-art [9,11,17] that moisture exposure leads to a significant reduction on the mechanical properties of epoxy resins, explicitly by reducing tensile strength and stiffness throughout the plasticization phenomenon. In order to measure the moisture absorption on specimens from EP3 series, 9 additional specimens (three specimens for each preparation method) were placed in the same hygrothermal condition during the creep test. The mass variation (mass increase divided by the initial mass) is depicted in Figure 9. After 2400 hours of exposure the mass variation on REF, V20 and V90 specimens was close to 0.93%, 0.66% and 0.65%, respectively. There is higher moisture absorption on the REF specimens, mainly because the degassing decreases the porosity of the adhesive. The hygrothermal condition of EP3 series can be assumed as an extreme environment and its consequent degradation effect accelerated the creep development on the epoxy adhesive. Consequently, the influence of the preparation method became more evident in test series EP3, and specimens prepared with the degassing procedure (V20 and V90) showed higher modulus of elasticity and smaller creep coefficient.

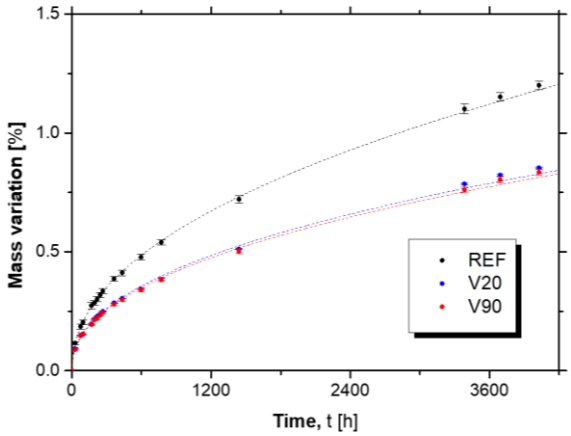

Figure 9. Mass variation over time for EP3 series.

Table 2 also presents the time for reaching the failure, t_{rup}, and the modulus of elasticity, E_{rup}, based on the instantaneous strain variation after rupture, $\Delta\varepsilon_{rup}$. The time for reaching the failure is higher in specimens with the degassing procedure (2142.6 hours) than on the REF specimens (1794.0 hours). At this final stage, V90 and V20 specimens present higher stiffness than the REF specimens, confirming, once again, that the preparation method has great influence on the mechanical behaviour of the epoxy adhesive. The E_{rup} is lower than the $E_{(t=0)}$ (reduction of 8.3%, 8.6% and 10.6% for REF, V20 and V90, respectively), which could be an indicator of the degradation effect of this extreme environment. It should be noted that the strain at failure on the creep tests was 35% to 59% higher than the ultimate strain obtained from the tensile tests. Similar behaviour was obtained by Costa and Barros [10], whom affirm that the adhesive is able to reorganize its internal structure during sustained loading.

3.3. Analytical modelling

To further understand the creep behaviour of all tested specimens, analytical modelling was carried out using, firstly, the Burgers model and, then, the modified Burgers model. The Burgers model is a rheological model widely used for the creep assessment of epoxy adhesives [7,10,25,26]. It is expressed by Equation (1):

$$\varepsilon_{creep}(t) = \sigma \cdot \left[\frac{1}{E_M} + \frac{t}{\eta_M} + \frac{1}{E_K} \cdot \left(1 - \exp\left(-\frac{E_K}{\eta_K} \cdot t\right)\right) \right] \quad (1)$$

where, $\varepsilon_{creep}(t)$, is the strain at a certain time instant, t; σ, is the applied creep stress; E_M, is the Maxwell's modulus of elasticity; η_M, is the Maxwell's coefficient of dynamic viscosity; E_K, is the Kelvin's modulus

of elasticity; η_K, is the Kelvin's coefficient of dynamic viscosity. Figure 10 illustrates the typical response when the Burgers model is used. In the Burgers model, the Maxwell's modulus of elasticity is inversely proportional to the elastic strain observed at the instance of loading, ε_M, and it is given by Equation (2):

$$E_M = \frac{\sigma}{\varepsilon_M} \tag{2}$$

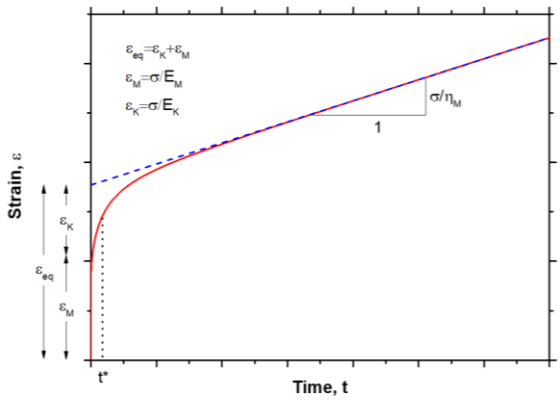

Figure 10. Strain evolution with time according to Burgers model.

The Maxwell's coefficient of dynamic viscosity is obtained from the steady-state branch of the creep curve. For the EP1 and EP2 series, the steady state branch was defined as the last third of the creep monitoring interval (from t = 1600 hours to t = 2400 hours), whereas for EP3 series, a shorter steady state interval was defined for each individual specimen. The steady-state branch is located at the secondary creep stage, when the creep strain variation with the time, ε'_M, is constant. The parameter η_K is obtained by Equation (3):

$$\eta_M = \frac{\sigma}{\varepsilon'_M} \tag{3}$$

The Kelvin's elastic modulus is obtained from the following Equation (4):

$$E_K = \frac{\sigma}{\varepsilon_{eq} - \varepsilon_M} = \frac{\sigma}{\varepsilon_K} \tag{4}$$

where the ε_{eq} is the value of strain obtained with the interception of the steady state branch (blue dashed line in Figure 10) with the vertical axis. The last parameter required in the definition of the Burgers

403 model, η_K, is obtained from the multiplication of the Kelvin's modulus of elasticity and the retardation
404 time, t^*, according to Equation (5):

$$\eta_K = E_K \cdot t^* \tag{5}$$

405 The retardation time is obtained from the exponential term from the Equation (1) and it corresponds to
406 the time required to reach 63.2% of the deformation accounted in the model by the Kevin-Voigt term, ε_K
407 (see Figure 10). To calculate the retardation time, the procedure adopted by Costa and Barros [5], was
408 followed: (i) isolate the Kevin-Voigt term from Equation (1), as given in Equation (6), (ii) subtract the
409 Maxwell terms ($\sigma/E_M + t \cdot \sigma/\eta_M$) from the experimental creep curve and then iii) determine the time
410 necessary to achieve 63.2% of ε_K (see Equation (4)).

$$\varepsilon_K(t) = \varepsilon_{creep}(t) - \left(\frac{\sigma}{E_M} + \frac{\sigma}{\eta_M} \cdot t\right) \tag{6}$$

411

412 Table 3 presents the Burgers model parameters computed for each specimen, whereas in Figure 11a the
413 relationship between numerical and experimental strain is presented for each series. Results showed good
414 correlations between the experimental and numerical results, with the maximum deviation close to 0.05%
415 of strain on EP2_REF_1. The mean absolute percentage deviation, *MAPD*, was computed to evaluate
416 the prediction accuracy of the Burgers model. The MAPD is calculated using the following expression:

$$MAPD = \frac{1}{N} \cdot \sum_{i=1}^{N} \left| \frac{\varepsilon_{exp,i} - \varepsilon_{num,i}}{\varepsilon_{exp,i}} \right| \tag{7}$$

417 where, *N*, is the number of sampling points (two points for each hour, for a minimum of 4800 points);
418 $\varepsilon_{exp,i}$, is the experimental strain measured at a sampling point *i*; and, $\varepsilon_{num,i}$, is the analytical strain obtained
419 for the sampling point *i*. The MAPD values are presented in Table 3.

420 For EP1 and EP2 series, an average MAPD value of 2.60% was obtained, whereas in EP3 series, the
421 average MAPD was equal to 3.26%. It should be noted that the Burgers model is used for the prediction
422 of the time-dependent strain within the first two (out of three) characteristic stages of creep. As referred
423 before, specimens from EP3 series experienced a full development of the tertiary creep stage and failure
424 during the creep loading. Therefore, the creep predictions using the Burgers model should deviate from
425 the experimental results for the final part of the test. Nevertheless, results showed that the Burgers model

426 can successfully predict the creep component of the epoxy adhesive, for each tested series. However, as
427 referred by Costa and Barros [10], the prediction of the experimental strains can be improved with the
428 introduction of a new parameter, *n*, in the exponential term from the Burgers model (Eq. (1)). In this
429 modified Burgers model, the time-dependent strain is obtained with the given Equation (8):

$$\varepsilon_{creep}(t) = \sigma \cdot \left[\frac{1}{E_M} + \frac{t}{\eta_M} + \frac{1}{E_K} \cdot \left(1 - \exp\left(\left(-\frac{E_K}{\eta_K} \cdot t \right)^{1-n} \right) \right) \right] \quad (8)$$

430
431 **Table 3:** Parameters used for the Burgers equation.

Series	Specimen	ε_M	ε'_M	ε_{eq}	ε_K	t*	E_M	η_M	E_K	η_K	MAPD
		[%]	[%/h]	[%]	[%]	[h]	[GPa]	[GPa·h]	[GPa]	[GPa·h]	[%]
EP1	EP1_REF_1	0.10	3.52e-05	0.29	0.19	56.25	8.78	24853	4.65	261.72	2.74
	EP1_REF_2	0.10	3.05e-05	0.27	0.17	65.15	8.37	280523	5.19	338.10	2.75
	EP1_V20_1	0.09	336e-05	0.24	0.15	56.67	12.4	34423	7.97	451.42	2.64
	EP1_V20_2	0.09	2.53e-05	0.22	0.13	64.91	12.2	443189	8.85	574.74	2.57
	EP1_V90_1	0.11	3.27e-05	0.25	0.15	61.28	12.0	39001	8.73	527.44	2.56
	EP1_V90_2	0.10	2.87e-05	0.25	0.15	65.37	12.6	44396	8.61	570.67	2.44
EP2	EP2_REF_1	0.08	3.25e-05	0.21	0.13	40.98	9.00	21132	5.21	213.32	2.69
	EP2_REF_2	0.07	2.78e-05	0.16	0.09	66.86	9.91	24718	7.37	492.89	2.57
	EP2_V20_1	0.07	1.96e-05	0.15	0.09	79.19	13.3	45457	10.4	821.21	2.53
	EP2_V20_2	0.07	2.29e-05	0.14	0.08	137.82	13.7	38880	11.3	1550.76	2.58
	EP2_V90_1	0.07	2.05e-05	0.16	0.09	80.39	13.2	47089	10.7	856.93	2.56
	EP2_V90_2	0.08	2.44e-05	0.17	0.10	82.25	12.9	39578	9.87	811.99	2.65
EP3	EP3_REF_1	0.10	1.63e-04	0.17	0.07	22.68	7.36	3716	14.0	248.69	3.24
	EP3_REF_2	0.10	2.23e-04	0.19	0.09	19.27	8.14	3201	10.2	178.01	2.71
	EP3_V20_1	0.08	0.67e-04	0.16	0.08	49.14	11.5	11471	13.9	608.54	4.14
	EP3_V20_2	--	--	--	--	--	--	--	--	--	--
	EP3_V90_1	0.08	0.98e-04	0.17	0.09	36.82	13.2	10239	11.3	415.56	1.36
	EP3_V90_2	0.08	1.06e-04	0.18	0.10	35.18	13.2	9080	11.9	399.19	2.00

ε_M – instantaneous elastic strain at the instance of loading; ε'_M – strain variation at the steady-state branch; ε_{eq} – strain obtained from the interception of the steady state branch with the vertical axis; ε_K – maximum strain obtained from the Kevin-Voigt term; ***t**** – time required to reach 63.2% of the ε_K; E_M – Maxwell's modulus of elasticity; η_M – Maxwell's coefficient of dynamic viscosity; E_K – Kelvin's modulus of elasticity; η_K – Kelvin's coefficient of dynamic viscosity; ***MAPD*** – mean absolute percentage deviation.

432
433 The parameter *n* of the modified Burgers model was computed by forcing the slope between the
434 numerical and experimental values, throughout the Generalized Reduced Gradient (GRG) nonlinear
435 function from Microsoft Excel. Table 4 presents the obtained *n* parameter of the modified Burgers model
436 for each tested specimen, and the corresponding result from the MAPD analysis. The relationship

437 between numerical and experimental strain is presented in Figure 11b for each series. The modified
438 Burgers model allowed a better prediction of the creep behaviour, with higher accuracy for the initial
439 stages of creep (see Figure 11b), confirmed with the reduction of the mean absolute percentage deviation.
440 Once again, the tertiary creep stage observed on EP3 series (after the 0.3% of strain) cannot be predicted
441 with the modified Burgers model, therefore, higher deviation between numerical and experimental
442 results are observed on these stages of test. The experimental and numerical curves (strain *versus* time)
443 are also presented in Figure 12. This figure shows great correlation between the experimental results and
444 the numerical model, with overlapping curves during the first and second creep stages (all 2400 hours
445 for EP1 and EP2 series, and up to 600 hours in EP3 series).

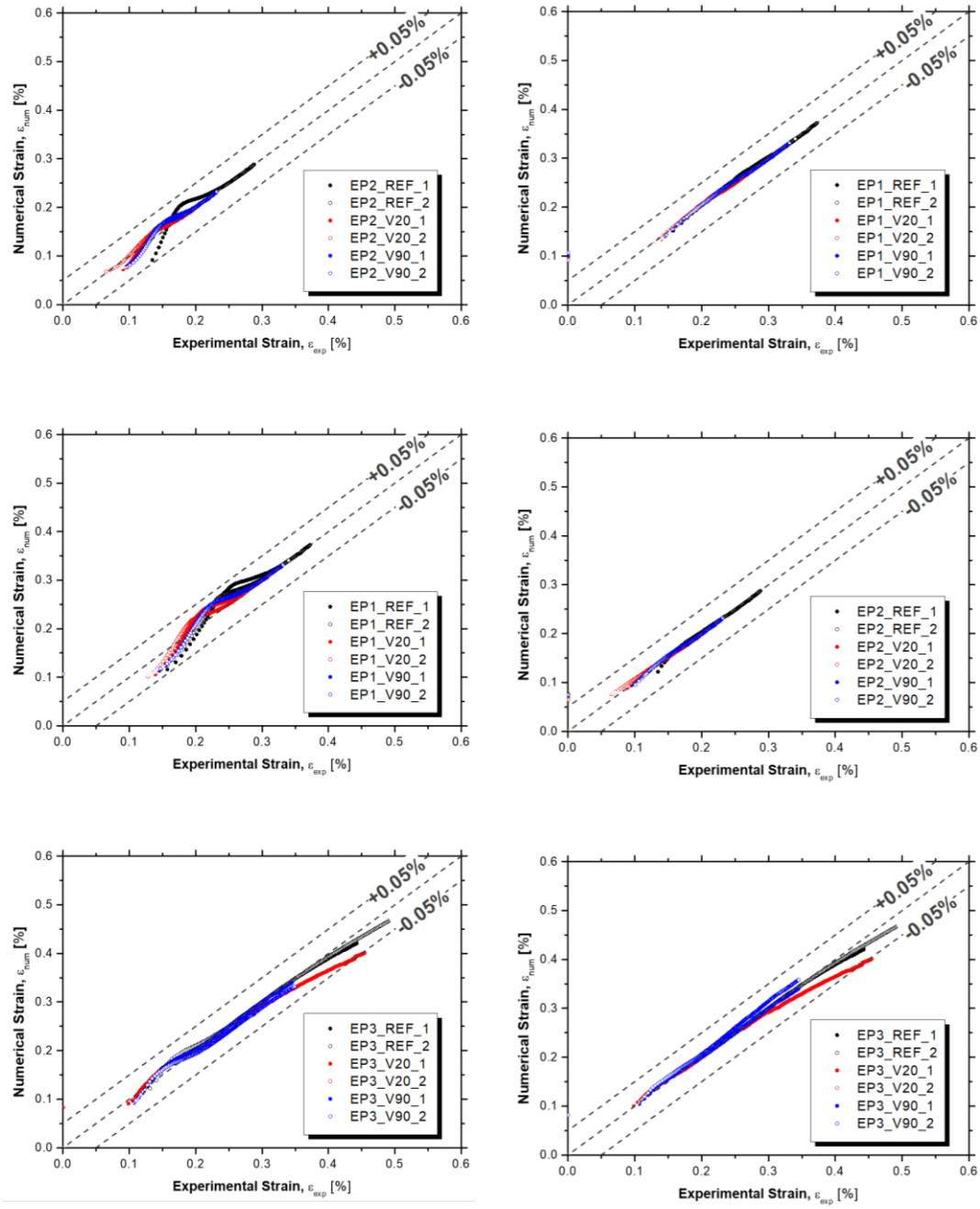

(a) (b)

Figure 11. (a) Relationship between Burgers model strain and experimental strain; (b) Relationship between modified Burgers model strain and experimental strain.

446

447 **Table 4:** Modified Burgers equation parameters.

Series	**Specimen**	**n**	**MAPD** [%]
EP1	EP1_REF_1	0.53	0.86
	EP1_REF_2	0.53	0.78
	EP1_V20_1	0.54	0.83
	EP1_V20_2	0.53	0.79
	EP1_V90_1	0.53	0.77
	EP1_V90_2	0.52	0.74
EP2	EP2_REF_1	0.59	0.85
	EP2_REF_2	0.52	0.92
	EP2_V20_1	0.50	0.83
	EP2_V20_2	0.42	1.54
	EP2_V90_1	0.49	0.93
	EP2_V90_2	0.48	0.99
EP3	EP3_REF_1	0.46	2.93
	EP3_REF_2	0.46	2.31
	EP3_V20_1	0.38	3.90
	EP3_V20_2	--	--
	EP3_V90_1	0.38	0.90
	EP3_V90_2	0.41	1.57

n – parameter from the modified Burgers model; ***MAPD*** – mean absolute percentage deviation.

448 From the analytical modelling it was possible to conclude that the values obtained for E_M, are highly
449 correlated with the instantaneous tensile properties, and show clear influence from the preparation
450 methods (see analysis on the $E_{(t=0)}$ on section 3.2). The Maxwell's coefficient of dynamic viscosity
451 defines the constant rate of creep strain variation (slop of the curve at the steady-state branch), with
452 higher values leading to lower slope on the creep curve. On EP1 and EP2 series the η_M is considerable
453 higher on the V20 and V90 specimens (average of 41642 GPa·h) than on REF specimens
454 (24688.82 GPa·h). On EP3 series the specimens with different preparation methods showed similar
455 trend, with lower values for the REF specimens. However, EP3 series present significant lower η_M
456 values, when compared with EP1 and EP2 series. This parameter not only indicate that the preparation
457 method has great influence on the creep development (when REF specimens are compared with V20 and
458 V90 specimens, an increase of 53%, 86% and 107% is obtained for EP1, EP2 and EP3 series, respectably)
459 but that the hygrothermal conditions from EP3 series lead to higher creep development, 3 to 9 times

460 higher than on EP1 and EP2 series, depending on the preparation method. The Kelvin's modulus of
461 elasticity shows the maximum creep strain developed from the Kevin-Voigt term, (ε_K) and the Kelvin's
462 coefficient of dynamic viscosity defines the development rate of ε_K. In EP1 and EP2 series, REF
463 specimens showed lower values for both parameters (E_K = 5.61 GPa and η_K = 326.51 GPa·h) than V20
464 and V90 specimens (E_K = 9.54 GPa and η_K = 770.65 GPa·h). EP3 series presents an average E_K of
465 12.25 GPa and the lowest average η_K (359.63 GPa·h) of all three series. It is noteworthy to stress that
466 there is low variation on the parameters from EP1 and EP2 series, for specimens with the same
467 preparation procedure. Based on the results from these two series, EP1 and EP2, it can be stated that this
468 material exhibits linear viscoelastic/viscoplastic tensile behaviour up to sustained stress levels of 40%.
469 Finally, two main conclusions can be drawn from the analytical model: (i) the preparation method has
470 great influence on the creep behaviour, with slower creep strain development for specimens subjected to
471 the degassing procedure; (ii) the hygrothermal conditions have high influence on the creep behaviour of
472 the adhesive, namely by increasing the slope of the creep curve on the steady-state branch (nearly 5.35
473 times higher).

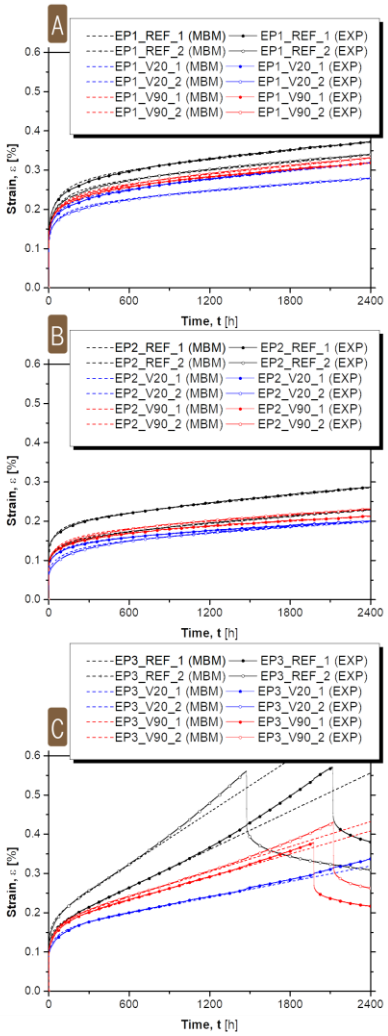

Figure 12. Experimental (EXP) strain *versus* time and modified Burgers model (MBM) strain *versus* time: (a) EP1 series; (b) EP2 series; and (c) EP3 series.

4. Conclusions

This paper presented and analysed the results from an experimental program aimed to further understand the tensile creep behaviour of a structural epoxy adhesive used for construction applications. New findings are added to the existing literature, namely at: (i) creep behaviour of epoxy adhesives manufactured using distinct processes of mixing (with and without degassing) and curing conditions (normal and accelerated); (ii) influence of hygrothermal conditions (98% of RH) on creep behaviour of epoxy prepared with different processes; and (iii) suitability of existing models to simulate the creep behaviour of epoxy adhesives prepared using different processes. The manufacturing procedure, curing conditions and the hygrothermal conditions were the main variables of this study. Based on the

484 experimental results, an analytical analysis was carried out using the Burgers and the modified Burgers
485 equations.
486 First, the tensile tests of epoxy adhesive demonstrated a significant increase on the instantaneous tensile
487 properties with the degassing procedure (V20 and V90). When compared with the reference specimens
488 (REF series), V20 specimens presented an increase on the average tensile strength and elastic modulus
489 of 31% and 41%, respectively, whereas the V90 specimens show an even higher growth of 45% and
490 49%, respectively.
491 In the creep tests, the instantaneous elastic strain observed at the instance of loading, $\varepsilon_{(t=0)}$, was consistent
492 with the quasi-static tensile tests. The hygrothermal conditions had great influence on the adhesive's
493 creep behaviour. Similar behaviour was observed for specimens from EP1 and EP2 series (20 ºC and
494 55% of relative humidity), with the development of creep up to the secondary creep stage in the
495 2400 hours of sustained loading. Specimens exposed to 20 ºC and 98% of relative humidity (EP3 series)
496 presented the development of all three stages of creep (primary, secondary and tertiary) up to failure
497 within the 2400 hours of test (exception for EP3_V20_1, where failure was obtained after 3628 hours of
498 loading).
499 An analytical analysis was carried out to further understand the creep behaviour of all tested specimens.
500 Two models were used: (i) the Burgers model and (ii) the modified Burgers model. Good correlations
501 between the experimental and the numerical results were obtained for both models. However, a better fit
502 was achieved with the latter model (average MAPD of 0.80%, 1.01% and 2.95% for EP1, EP2 and EP3
503 series, respectively) than in with the Burgers model (average MAPD of 2.62%, 2.60% and 3.26% for
504 EP1, EP2 and EP3 series, respectively).
505 The analysis on the creep parameters E_M; η_M; E_K; and η_K, showed that the preparation method has great
506 influence on the creep behaviour, with slower creep strain development for specimens subjected to the
507 degassing procedure. This analysis also showed that the hygrothermal conditions have high influence on
508 the creep behaviour of the adhesive, namely with the relative humidity increase (from 55% on EP1 and
509 EP2 series to 98% on EP3 series), the slope of the creep curve on the steady-state branch was 5.35 times
510 higher. Finally, in EP1 and EP2 series, specimens with the same preparation procedure exhibit linear
511 viscoelastic/viscoplastic tensile behaviour up to sustained stress levels of 40%.
512

5. Acknowledgements

This work was carried out in scope of the project FRPLongDur POCI-01-0145-FEDER-016900 (FCT PTDC/ECM-EST/1282/2014) funded by national funds through the Foundation for Science and Technology (FCT) and co-financed by the European Fund of the Regional Development (FEDER) through the Operational Program for Competitiveness and Internationalization (POCI) and the Lisbon Regional Operational Program and, partially financed by the project POCI-01-0145-FEDER-007633. This work was also partly financed by FCT / MCTES through national funds (PIDDAC) under the R&D Unit Institute for Sustainability and Innovation in Structural Engineering (ISISE), under reference UIDB/04029/2020. The authors also like to thank the S&P Clever Reinforcement Ibérica Lda. company for providing the materials. The first author wishes also to acknowledge the grant SFRH/BD/131259/2017 provided by Fundação para a Ciência e a Tecnologia (FCT), while the fourth author acknowledge his sabbatical grant SFRH/BSAB/150266/2019, provided by FCT, financed by European Social Fund and by national funds through the FCT/MCTES.

6. References

[1] FIB. Externally applied FRP reinforcement for concrete structures. 2019.

[2] ACI 440.2R-08. Guide for the design and construction of externally bonded FRP systems for strengthening existing structures. 2008.

[3] Sena-Cruz JM, Barros JAO, Coelho MRF, Silva LFFT. Efficiency of different techniques in flexural strengthening of RC beams under monotonic and fatigue loading. Constr Build Mater 2012;29:175–82. https://doi.org/10.1016/j.conbuildmat.2011.10.044.

[4] Correia L, Sena-Cruz J, Michels J, França P, Pereira E, Escusa G. Durability of RC slabs strengthened with prestressed CFRP laminate strips under different environmental and loading conditions. Compos Part B Eng 2017;125:71–88. https://doi.org/10.1016/j.compositesb.2017.05.047.

[5] Correia L, Teixeira T, Michels J, Almeida JAPP, Sena-Cruz J. Flexural behaviour of RC slabs strengthened with prestressed CFRP strips using different anchorage systems. Compos Part B Eng 2015;81:158–70. https://doi.org/10.1016/j.compositesb.2015.07.011.

[6] Sena-Cruz J, Michels J, Harmanci YE, Correia L. Flexural strengthening of RC slabs with

542 prestressed CFRP strips using different anchorage systems. Polymers (Basel) 2015;7:2100–18.
543 https://doi.org/10.3390/polym7101502.
544 [7] Silva P, Valente T, Azenha M, Sena-Cruz J, Barros J. Viscoelastic response of an epoxy adhesive
545 for construction since its early ages: Experiments and modelling. Compos Part B Eng
546 2017;116:266–77. https://doi.org/10.1016/j.compositesb.2016.10.047.
547 [8] Michels J, Sena-Cruz J, Christen R, Czaderski C, Motavalli M. Mechanical performance of cold-
548 curing epoxy adhesives after different mixing and curing procedures. Compos Part B Eng
549 2016;98:434–43. https://doi.org/10.1016/j.compositesb.2016.05.054.
550 [9] Sousa JM, Correia JR, Cabral-Fonseca S. Durability of an epoxy adhesive used in civil structural
551 applications. Constr Build Mater 2018;161:618–33.
552 https://doi.org/10.1016/j.conbuildmat.2017.11.168.
553 [10] Costa I, Barros J. Tensile creep of a structural epoxy adhesive: Experimental and analytical
554 characterization. Int J Adhes Adhes 2015;59:115–24.
555 https://doi.org/10.1016/j.ijadhadh.2015.02.006.
556 [11] Cabral-Fonseca S, Correia JR, Custódio J, Silva HM, Machado AM, Sousa J. Durability of FRP
557 - concrete bonded joints in structural rehabilitation: A review. Int J Adhes Adhes 2018;83:153–
558 67. https://doi.org/10.1016/j.ijadhadh.2018.02.014.
559 [12] Moussa O, Vassilopoulos AP, Keller T. Effects of low-temperature curing on physical behavior
560 of cold-curing epoxy adhesives in bridge construction. Int J Adhes Adhes 2012;32:15–22.
561 https://doi.org/10.1016/j.ijadhadh.2011.09.001.
562 [13] Moussa O, Vassilopoulos AP, de Castro J, Keller T. Early-age tensile properties of structural
563 epoxy adhesives subjected to low-temperature curing. Int J Adhes Adhes 2012;35:9–16.
564 https://doi.org/https://doi.org/10.1016/j.ijadhadh.2012.01.023.
565 [14] Czaderski C, Martinelli E, Michels J, Motavalli M. Effect of curing conditions on strength
566 development in an epoxy resin for structural strengthening. Compos Part B Eng 2012;43:398–
567 410. https://doi.org/10.1016/j.compositesb.2011.07.006.
568 [15] Michels J, Widmann R, Czaderski C, Allahvirdizadeh R, Motavalli M. Glass transition
569 evaluation of commercially available epoxy resins used for civil engineering applications.
570 Compos Part B Eng 2015;77:484–93.

571 [16] Savvilotidou M, Vassilopoulos AP, Frigione M, Keller T. Development of physical and
572 mechanical properties of a cold-curing structural adhesive in a wet bridge environment. Constr
573 Build Mater 2017;144:115–24. https://doi.org/10.1016/j.conbuildmat.2017.03.145.
574 [17] Silva P, Fernandes P, Sena-Cruz J, Xavier J, Castro F, Soares D, et al. Effects of different
575 environmental conditions on the mechanical characteristics of a structural epoxy. Compos Part
576 B Eng 2016;88:55–63. https://doi.org/10.1016/j.compositesb.2015.10.036.
577 [18] S&P. Technical Data Sheet S & P Resin 220 epoxy adhesive. Seewen, Switzerland: 2012.
578 [19] EN 12190:1999. Products and systems for the protection and repair of concrete structures. Test
579 methods. Determination of compressive strength of repair mortar 1999.
580 [20] International Organizational for Standardization. ISO 178:2002 - Plastics -- Determination of
581 flexural properties. Hanser 2002.
582 [21] BS EN 12615:1999. Products and systems for the protection and repair of concrete structures.
583 Test methods. Determination of slant shear strength 1999.
584 [22] International Organization for Standardization. ISO 527-2:2012 - Plastics — Determination of
585 tensile properties — Part 2: Test conditions for moulding and extrusion plastics. Geneva: 2012.
586 [23] International Organization for Standardization. ISO 527-1:2012 - Plastics -- Determination of
587 tensile properties -- Part 1: General principles. Geneva 2012.
588 [24] Granja JL, Fernandes P, Benedetti A, Azenha M, Sena-Cruz J. Monitoring the early stiffness
589 development in epoxy adhesives for structural strengthening. Int J Adhes Adhes 2015;59:77–85.
590 https://doi.org/https://doi.org/10.1016/j.ijadhadh.2015.02.005.
591 [25] Majda P, Skrodzewicz J. A modified creep model of epoxy adhesive at ambient temperature. Int
592 J Adhes Adhes 2009;29:396–404. https://doi.org/10.1016/j.ijadhadh.2008.07.010.
593 [26] Godzimirski J, Rośkowicz M. Numerical analysis of long-lasting strength of adhesive bonds.
594 Adv Manuf Sci Technol 2004;28:67–83.
595